Journal of Water Process Engineering 74 (2025) 107681

Contents lists available at ScienceDirect

Journal of Water Process Engineering

journal homepage: www.elsevier.com/locate/jwpe

Phosphorus retention and hydraulic performance in borrow sand-based wastewater soil treatment units in impermeable settings: Case study in Abitibi-Témiscamingue, Québec

Sorour Sheibani [a,*], Michelle Nasrallah [a], Benoît Courcelles [a], Eric Rosa [b], Brahim Maylal [b], Dominique Claveau-Mallet [a]

[a] Department of Civil, Geological & Mining Engineering, Polytechnique Montréal, 2900 Boulevard Édouard-Montpetit, Montréal, Québec H3T 1J4, Canada
[b] Groundwater Research Group (GRES), Research Institute on Mines and Environment (RIME), Université du Québec en Abitibi-Témiscamingue (UQAT), 341 Rue Principale N, Amos, Québec J9T 2L8, Canada

ARTICLE INFO

Editor: Guangming Jiang

Keywords:
Septic system within impermeable soils
Water saturation
Phosphorus elimination
Field inspection
COMSOL Multiphysics numerical simulations

ABSTRACT

On-site wastewater treatment systems (OWTS), including soil treatment units (STUs), rely on effluent infiltration into local soils for treatment. However, in regions with impervious soils, this process becomes challenging. As a result, borrow sand is necessary for STU construction. For example, in the Abitibi-Témiscamingue region (western Québec, Canada), impervious sediments from the Clay Belt necessitate the use of such systems. This study evaluates the hydraulic performance and phosphorus retention capacity of borrow sand-based STUs through field inspections, laboratory experiments, and numerical modelling. Field inspections of 26 septic systems revealed that only 2 systems exhibited surface flooding, suggesting minimal hydraulic failure. However, sampling from 12 systems showed that 9 released phosphorus into the environment, with phosphorus concentrations exceeding 35 mg/L in the downstream ditches in some cases, which were far above Québec's surface water limit of 0.03 mg/L. Laboratory sorption tests demonstrated that the sands used in STUs had limited maximum P sorption capacities (88.49 and 17.12 mg/kg). Numerical simulations using COMSOL Multiphysics further indicated that P retention in the sand layer is likely to be exhausted within a year, leading to P migration into the environment. Simulations also indicated that systems with properly designed outlets to a drainage ditch could maintain hydraulic performance during extreme rainfall events. These findings highlight the inadequacy of current borrow sand-based STU designs in ensuring long-term phosphorus retention. To mitigate environmental contamination, improved design strategies and management practices should be considered.

1. Introduction

In sparsely populated areas, residences are not connected to centralized wastewater treatment plants. Instead, domestic wastewater is treated in decentralized onsite wastewater treatment systems (OWTSs). In a conventional OWTS, primary treatment takes place in a septic tank, and secondary treatment occurs in a downgradient soil treatment unit (STU) such as a drain field. However, if wastewater is not properly treated, septic systems can introduce contaminants such as organic chemicals, nutrients (phosphorus and nitrogen), and pathogens into the environment (e.g. [1,2]). In Canada, approximately 25 % of the population uses septic systems for wastewater treatment [3], highlighting the importance of monitoring their performance.

In regions with clayey soils, including Canada's Clay Belt—covering 180,000 km^2 across Ontario and Québec—traditional STUs face significant challenges. These impervious soils restrict infiltration, reducing the effectiveness of treatment. In such environments, STUs constructed with borrow sand offer a practical solution to improve infiltration and wastewater treatment. For these systems to perform effectively, the unsaturated zone must facilitate oxygen diffusion, supporting aerobic microbial activity and the oxidation of pollutants such as organic carbon (e.g. [4]). However, the impermeability of the underlying soils makes the design of the effluent discharge path crucial for maintaining hydraulic efficiency and preventing water accumulation or flooding.

Different designs have been developed for borrow sand-based STUs to address site-specific challenges. The University of Wisconsin, for

* Corresponding author.
E-mail address: sorour.sheibani@polymtl.ca (S. Sheibani).

https://doi.org/10.1016/j.jwpe.2025.107681
Received 10 January 2025; Received in revised form 13 March 2025; Accepted 6 April 2025
Available online 22 April 2025

example, developed an aboveground mound system using borrow coarse sand, which can be installed in both permeable and impermeable settings. These systems discharge effluent through infiltration into the soil and, when properly designed, prevent ponding and side seepage [5]. In Nova Scotia, sand filters are constructed with borrow fine and coarse sand in impermeable areas, with effluent either infiltrating the soil or discharging to the surface, depending on site conditions and system design [6]. Previous field studies suggest that the performance of onsite wastewater treatment systems in Nova Scotia is acceptable in terms of the elimination of biological oxygen demand (BOD) which suggests sufficient unsaturated depth [7]. Nevertheless, the hydraulic performance of STUs inevitably depends on local climatic and hydrogeological conditions. Consequently, further studies need to be conducted in various settings to test the applicability of treatment approaches and assess optimal design features. Moreover, the increase in recent intense rainfall events driven by climate change [8], puts extra pressure on borrow sand-based STUs —a factor largely overlooked in existing designs. Therefore, studying the effective hydraulic performance of STUs has become crucial for enhancing resilience and ensuring reliable operation.

Phosphorus (P) is of particular concern in wastewater due to its role in eutrophication. Even small concentrations, as low as 0.03 mg/L, can trigger eutrophication in surface water [9]. Studies confirm that septic systems contribute to P pollution in surface water bodies (e.g., [10,11]). A small amount of particulate P (typically 20 to 30 % of total P) is removed in septic tanks during sludge settling [12–14]. However, most dissolved P, primarily as orthophosphate, moves into the drain field, where it may be taken up by plants, interact with soil through sorption and precipitation, or migrate toward groundwater through advection-dispersion processes [2]. Sorption and precipitation, depending on the presence of positively charged ions and pH, are the primary physiochemical mechanisms leading to P elimination in STUs [15]. Unlike STUs in naturally permeable soils where deeper layers contribute to P adsorption, borrow sand systems rely entirely on the finite adsorption capacity of the sand layer.

Researchers have studied the suitability of sandy STUs in P removal through various approaches. Laboratory studies highlight the variability of P removal. Hamisi et al. [16] reported an average P removal of about 80 % in 0.6 m long sand-based columns operated for 300 days at a hydraulic load of 0.011 m/d. In contrast, Wang et al. [17] found that P removal declined rapidly in 0.3 m sand filters as adsorption sites became saturated. P removal in their study ranged from 24 to 32 % at higher hydraulic loads (0.049 m/d) and improved to 35 to 53 % at lower loads (0.024 m/d), with complete breakthrough occurring in <75 days.

There are a few multi-site studies on real systems operating over the long term that also demonstrate contrasting outcomes. Robertson et al. [18] investigated 24 OWTSs in Ontario, ranging from 8 to 45 years old, through plume monitoring. Their studied systems achieved an average P removal efficiency of 80 %, which was attributed to mineral precipitation mechanisms and favorable soil chemistry. Among these systems, 10 were built on clay or granitic bedrock, relying on imported, medium-coarse sand with 9 achieving over 75 % P retention. In contrast, Eveborn et al. [19] documented long-term failure, with P removal declining to around 12 % in four sand-based STUs after 14 to 22 years of operation due to the saturation of adsorption sites. Their approach included sampling the filter beds and analysis of accumulated P. Similarly, Eveborn et al. [20] evaluated six OWTSs (11 to 28 years old) in Sweden, four of which used imported sand over clay soils. They estimated removal rates below 30 %. None of the abovementioned studies included investigations on the hydraulic performance of the systems.

Given the variability in P removal reported in previous studies and the limited research on the hydraulic performance and outlet design of systems within infiltration-preventive natural settings, further research is essential to understand how site-specific factors, material availability, design choices, and management practices influence the performance of borrow sand-based STUs. To our knowledge, this study is the first investigation to deepen the understanding of STUs built with borrow sand over clayey soils, focusing on both hydraulic performance and P removal. The reference area for this study is the Abitibi-Témiscamingue region, where many isolated households rely on OWTSs due to the rural setting. The widespread use of private wells for drinking water in this area further underscores the importance of preventing contamination from improperly treated septic effluent.

A novel, multi-faceted approach was employed to assess hydraulic performance and P removal efficiency, incorporating multi-site field inspections to identify STUs' failure risks in terms of P releases and flooding. To better understand the factors driving performance, the study included characterization of natural soils, laboratory tests to evaluate the adsorption capacity of two sands suitable for STU construction, and numerical simulations modelling P transport and water saturation across various real-world design scenarios. The new numerical framework integrates climate change considerations by simulating extreme rainfall events. Beyond performance evaluation, this study introduces a broadly applicable methodological framework for assessing site conditions and modelling wastewater treatment outcomes, offering practical guidance for the design, construction, and management of STUs in challenging environmental settings.

2. Methodology

2.1. Site description

The reference area of this study, the Abitibi-Témiscamingue region in western Québec, is depicted in Fig. 1a along with silt and clay coverings. The hydrogeological environment of the study area is described in detail by Cloutier et al. [21–23] and Nadeau et al. [24,25]. Fine-grained glaciolacustrine sediments of Lake Barlow-Ojibway are found in this region. These varved sediments (centimetric alternations of subhorizontal layers of clay and silt) can reach thicknesses of over 50 m and cover over 38 % of the region's municipalized territory [23].

The information regarding the original soil types (Fig. 1b) and locations (Fig. 1c) of 223 septic systems within the study area were obtained from municipal records. The aim was to study a large pool of data to establish the general context of septic systems in the study area. STUs of these systems are relevant to the septic installations addressed in this study. Soil types were defined based on the permeability categories defined by Québec's guidelines, further explained in the supplementary information (SI), Section 1. While a total of 14 % of the studied systems were built in very permeable, permeable, and lowly permeable soils, 82 % of the systems were built in impermeable soils (Fig. 1b). The presence of lakes and rivers in Fig. 1c vulnerable to eutrophication highlights the importance of P removal as a key objective. Additionally, in Québec, OWTSs' regulations prioritize P as the limiting nutrient of the local ecosystems.

In a conventional septic system, a septic tank is followed by a drain field, as shown in Fig. 2a. However, more advanced septic systems include additional treatment steps. The target septic systems in Abitibi-Témiscamingue are advanced systems built in impermeable soil. Since the natural soil does not support infiltration, these systems include STUs as polishing fields constructed with borrow sand and are further classified into 3 categories based on the treatment chains.

In all studied systems, treatment chains start with a septic tank. Following this, some systems include a sand filter (Category 1), or an advanced secondary treatment system (Category 2). Other systems incorporate an advanced secondary treatment system superimposed to a polishing field (Category 3). All systems ultimately discharge into borrow-sand based polishing fields. In some septic systems, ditches were present downgradient of the polishing bed. The treatment chains in these 3 categories are illustrated in Fig. 2b, c and d. As shown in Fig. 1b, among all 223 systems, 80 % were installed in impermeable soil with borrow sand STUs, following one of the specified categories. The proportions of each system category are also shown in Fig. 1b.

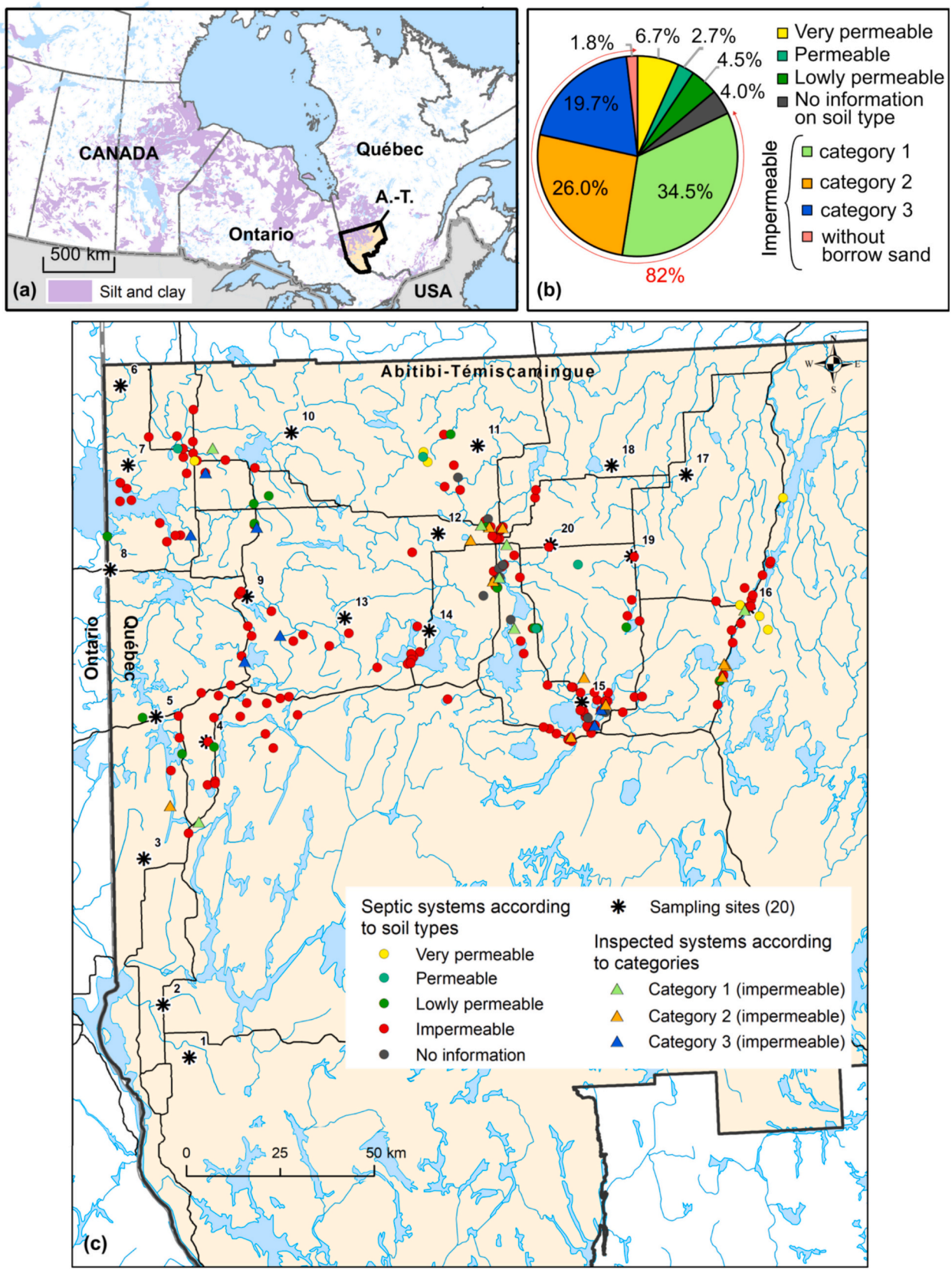

Fig. 1. (a) Map of Abitibi-Témiscamingue in Québec, Canada and silt and clay coverings [54-56]. (b) Classification of documented systems based on soil type and system category, (c) Location of documented systems with their settings' permeability, sampling sites and inspected systems.

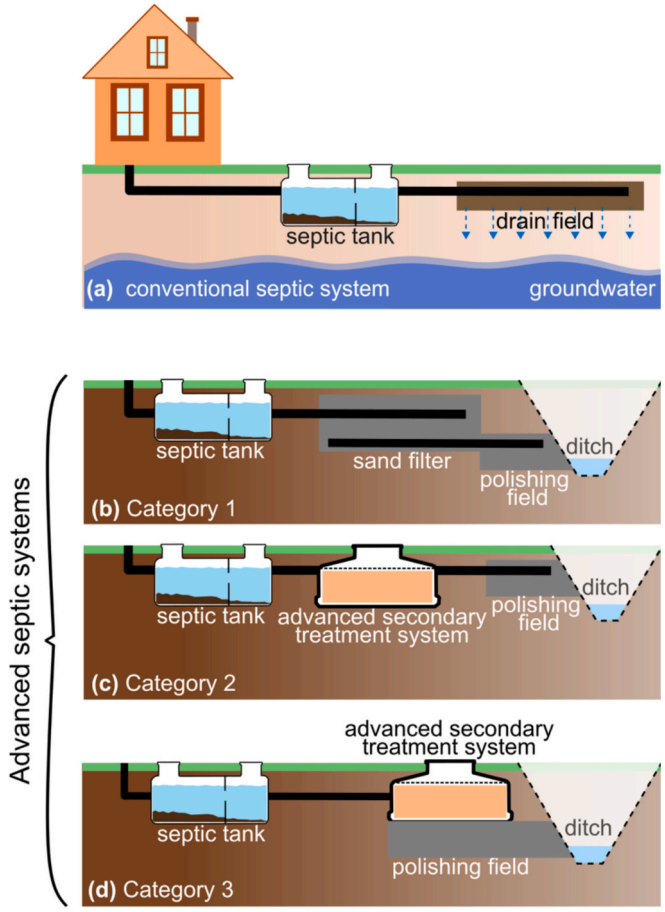

Fig. 2. Schematic representation of septic system treatment chains. (a) Conventional septic system with a drain field. (b–d) Advanced septic systems found in Abitibi-Témiscamingue, which are constructed in impermeable soils and include a borrow-sand-based polishing bed. These systems are categorized into three types based on their treatment chain: (b) Category 1 — septic tank + sand filter + polishing bed, (c) Category 2 — septic tank + advanced secondary treatment + polishing bed, and (d) Category 3 — septic tank + advanced secondary treatment superimposed onto a polishing bed.

In comparison with a drain field, a polishing field is smaller in thickness and area but receives larger hydraulic loading rates [L/m^2/d]. Polishing fields and drain fields are constructed in trenches or infiltration beds [26]. Here, the studied polishing fields were built as polishing beds.

2.2. Field sanitary inspections

Sanitary inspections were conducted from July to August 2022. Twenty-six residences with septic systems including borrow sand polishing beds leading to ditches were targeted. These septic systems were chosen to encompass a variety of characteristics to reflect real-world conditions within the study area. The studied systems spanned all three main categories shown in Fig. 2, with sizes ranging from 7 to 32 m^2, estimated hydraulic loads from 0.27 to 1.62 m^3/d (0.025 to 0.077 m/d), and ages between 2 and 17 years. They also included different inlet distribution methods, either gravity-fed or low-pressure systems. Further details about the inspected systems are provided in Table S1 of the SI. Gravity-fed systems and low-pressure systems are the main types of distribution of influent to soils in STUs [27] and were further explained in the SI, Section 4.

The hydraulic loads of the systems were estimated based on the number of residents and the wastewater production of 0.27 m^3/d per person [27]. The average occupancy rate, defined as the ratio of produced wastewater discharge to the system's full capacity according to local regulations [27], was 45 % in the inspected systems.

Septic systems were inspected for any sign of hydraulic failure (such as flooding). Water samples from ditches were collected at 2 points: (i) where polishing beds lead to ditches, and (ii) 5–10 m upstream from the polishing fields only if enough flow existed in the ditches. The plan of the sampling points is shown in Fig. S2 of the SI. All samples were collected in triplicate. The location and categories of the inspected systems are shown in Fig. 1c.

Samples were analyzed for total P concentration according to MELCCFP [28]. In short, samples were collected in plastic bottles and acidified to pH < 2 and then shipped to the laboratory and stored at 4 °C. Next, samples were aliquoted into assay tubes, alongside standards and controls. Each tube received 120 µL of saturated potassium persulfate and was subjected to digestion in an autoclave and then cooled and assayed for absorbance.

The amount of released P was calculated as the difference in the average concentration of total P in the two sampling points as follows:

$$\text{Released P} = P_{polishing\ bed} - P_{upstream} \quad (1)$$

where $P_{polishing\ bed}$ [mg/L] and $P_{upstream}$ [mg/L] are the average total P concentrations at the level of polishing beds and upstream of the polishing beds respectively.

2.3. Sampling and analysis of natural soils

During the Fall of 2021, natural soil samples were collected at 20 sites covering several municipalities in Abitibi-Témiscamingue. The sampling points were not directly associated with individual septic systems but were chosen across the study area to capture the spatial variability of the clay deposit at the regional scale (sites shown in Fig. 1c). At each site, 55 cm of the soil was excavated with an auger at first. Samples were then collected at depths of 55 cm to 70 cm also using an auger and weighed in the field. This depth corresponds to the approximate depth at which the STUs are constructed, ensuring that the soil characteristics at the relevant depth were studied. The procedure was repeated several times until 4 kg composite samples were obtained from each site. Samples were stored in tightly sealed plastic sampling bags, placed in rigid plastic buckets and carried to the Polytechnique Montreal geotechnical laboratory. All samples were stored in a refrigerator with humidity control prior to the tests.

The grain size distribution of samples was evaluated through sieve analyses conducted according to ASTM C136 [29] and clay content was estimated as the mass portion of particles smaller than 0.002 mm [30]. Additionally, the soil type was determined according to Quebec's regulations [27], further explained in the SI, Section 1.

2.4. Adsorption batch test

The adsorption tests were carried out on two sands that were likely to be used for the construction of the target STUs, to further investigate the factors influencing their performance in P removal. The first sand, identified as S1, comes from a quarry located in the city of Rouyn-Noranda in Abitibi-Témiscamingue, aligning with local resource availability and regional practices. The second sand, S2, is used in the preparation of concrete, further reflecting the types of sands commonly available and suitable for construction.

These two sands met the following criteria based on the regional regulations: (i) an effective particle size, d_{10}, between 0.25 and 1 mm, (ii) a uniformity coefficient, Cu, ≤4.5, (iii) <3 % of particles smaller than 80 µm, and (iv) <20 % of the particles larger than 2.5 mm [26]. Further justifications on S1 and S2 meeting the specifications are presented in the SI, Section 5.

Municipal wastewater often carries between 4 and 16 mg P/L [31]. Here, solutions with P concentrations of 2, 5, 10, 15 and 20 mg/L, which

covers a realistic range, were prepared by diluting a 100 mg P/L solution of KH_2PO_4 in Milli-Q water. In all solutions, 0.1 M potassium nitrate (KNO_3) was also added to maintain a constant conductivity of approximately 10 μS/cm [15].

The adsorption tests were carried out according to the ASTM D4646 standard [32]. Sands were spread in a layer of 2–3 cm and air-dried for 7 days until a constant weight was achieved. Subsequently, 2 g of sand was added to the P solutions at a media/solution mass ratio of 1:20. Blank samples (P solutions with no sand) with the same concentrations were also tested. All samples were then placed in a rotary extractor for 24 h at a speed of 29 rpm, at a room temperature of 22 °C. After 24 h of agitation, the samples were allowed to settle for 1 h. Then, samples were filtered through Whatman GF/C filters (47 μm), and P concentrations were measured according to the USEPA PhosVer® 3 ascorbic acid method. The pH of all samples was measured before and after the test.

2.4.1. Isotherm modelling

Following the adsorption batch test, Freundlich and Langmuir isotherm equations were fitted to the adsorbed and equilibrium P concentrations. Freundlich's equation is:

$$c_a = k_F c^{b_F} \tag{2}$$

where c_a is the equilibrium mass of the adsorbate (P) per unit mass of adsorbent [g/kg], c is the adsorbate (P) concentration [mg/L] at equilibrium, and k_F [(g/kg) $(mg/L)^{-b_F}$] and b_F [−] are constants. Langmuir's equation is:

$$c_a = \frac{ck_L b_L}{1 + cb_L} \tag{3}$$

where k_L [g/kg] and b_L $[mg/L]^{-1}$ are constants. k_L denotes the maximum Langmuir adsorption capacity and b_L is related to the binding energy.

2.5. Numerical modelling

2.5.1. Conceptual model, simulation scenarios and boundary conditions

In the polishing beds studied here, perforated pipes were placed in a layer of crushed stone within the borrow sand leading to a ditch (Fig. 3). Water flow and P transport were modeled for different polishing beds (Table 1). General properties of all models were derived from the real systems in the study area. Additionally, the simulated models were designed to incorporate the range of variability observed in these systems. These variabilities include factors such as STU size, occupancy rates, shape (rectangular or square), and the adsorption capacity of the borrow sand used.

According to local criteria, the area of each polishing bed is based on the number of bedrooms in the residence, with larger residences requiring larger polishing beds [26]. To account for variation in size, the models include residences with 1 to 6 bedrooms. In all models, the areas of polishing beds were directly taken from local regulations [26]. We considered two occupancy rates: 100 % occupancy, representing full capacity, and 45 % occupancy, which is the average local rate. The occupancy rate directly affects the influent discharge to the polishing beds. Based on the local regulation, the maximum discharge, applied at 100 % occupancy, is 0.54 m^3/d for a 1-bedroom residence and 3.24 m^3/d for a 6-bedroom residence [26]. For 45 % occupancy, the influent discharge is calculated as the product of the occupancy rate and the maximum inlet discharge.

Rectangular and square polishing beds were simulated for 6-bedroom residences to account for shape-related differences. In rectangular models, the width of the bed was set at 2.4 m to accommodate two pipes, and the length was calculated based on the required area. In square models, the width and length were equal, matching the total required area.

Model 1 represents the polishing bed for a 1-bedroom residence. Model 2 is a rectangular polishing bed for a 6-bedroom residence, with the same width as Model 1 but a longer length. Model 3 simulates a square polishing bed for a 6-bedroom residence to evaluate the effect of bed shape on performance. Models 4–6 replicate Models 1–3 but with 45 % occupancy to account for the average occupancy rate identified during field inspections. Models 7–12 follow the same configuration as Models 1–6 but use S2 sand, which has a different P sorption capacity compared to the S1 sand used in the first six models.

In Models 1–12, average rainfall intensity was considered. To assess the hydraulic performance under extreme conditions, three additional

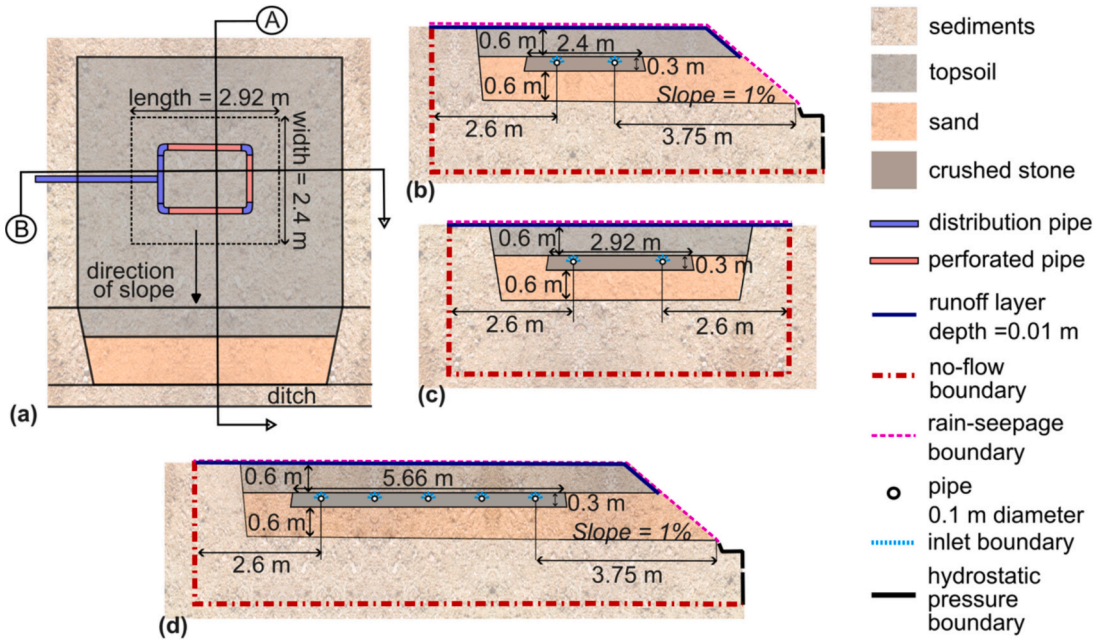

Fig. 3. Simulated polishing beds and the implemented boundary conditions. (a) Plan of a polishing bed for 1-bedroom residences. The dashed line shows the boundaries of the crushed stone layer. (b) Cross-section A simulated for polishing beds for 1-bedroom residences and rectangular polishing beds for 6-bedroom residences. (c) Cross-section B considered for 3D simulation of model 1. (d) Cross-section simulated for all square polishing beds for 6-bedroom residences.

Table 1
Characteristics of simulated polishing beds (number of bedrooms of residences, polishing bed area, occupancy rate, influent discharge, with of polishing bed, sand type, and rainfall intensity).

Model number	Number of bedrooms	Polishing bed area, A_p [m^2]	Occupancy rate (%)	Influent discharge, Q_{inf} [m^3/d]	Width of polishing bed [m]	Sand type	Rainfall [mm/d]
1*	1	7	100	0.54	2.4	S1	2.5
2	6	32	100	3.24	2.4	S1	2.5
3	6	32	100	3.24	5.66	S1	2.5
4	1	7	45	0.24	2.4	S1	2.5
5	6	32	45	1.46	2.4	S1	2.5
6	6	32	45	1.46	5.66	S1	2.5
7	1	7	100	0.54	2.4	S2	2.5
8	6	32	100	3.24	2.4	S2	2.5
9	6	32	100	3.24	5.66	S2	2.5
10	1	7	45	0.24	2.4	S2	2.5
11	6	32	45	1.46	2.4	S2	2.5
12	6	32	45	1.46	5.66	S2	2.5
13	1	7	100	0.54	2.4		78
14	6	32	100	3.24	2.4		78
15	6	32	100	3.24	5.66		78

* Simulated in both 2D and 3D.

models (Models 13–15) were included. These models exclude P transport and are subjected to torrential rainfall events to evaluate system performance under intense precipitation.

Two-dimensional models are frequently preferred to their 3-dimensional counterparts due to their less computational costs. Researchers usually apply dimensional contraction along the dimension in which the quantity of interest varies negligibly [33]. To the best knowledge of the authors, modelling STUs is generally done in 1D and 2D (e.g., [34,35]). Here, in the case of dipping polishing beds, 2D simulations can be used to predict hydraulic integrity and the fate of contaminants. The reason is that wastewater disperses uniformly in the crushed stone layer and moves through the sand layer in the direction of the slope with negligible flow perpendicular to the slope. Therefore, for all 15 models, 2D simulations were performed. To further justify the use of 2D modelling, model 1 was simulated in 3D and compared to its 2D equivalent in the SI, Section 7. This approach led to the validation of 2D modelling in the context of this study.

Fig. 3a represents the plan of a polishing bed for a 1-bedroom residence and Fig. 3b and c exhibit cross-sections A and B. The surface area of the crushed stone layer corresponds to polishing bed's area. The crushed stone layer in cross-sections A and B represents the width and length of the polishing bed, respectively. Cross-section A is in the direction of the slope and was simulated for 2D models with 1 bedroom. The 3D simulation of model 1 was then conducted considering the geometry of both cross-sections. Rectangular polishing beds designed for 6-bedroom houses have the same width as 1-bedroom models (Table 1), therefore the cross-section of Fig. 3b was simulated using the same geometry. Finally, the cross-section in Fig. 3d was designed for square polishing beds associated with 6 bedrooms. The plans of polishing beds designed for 6-bedroom residences are provided in Fig. S4 of the SI.

For models 1–12, simulations were performed in two steps. First, an average rainfall intensity of 2.5 mm/day, as suggested by Labonté-Raymond et al. [36], was implemented, until a steady state was obtained. In the second step, the inflow from perforated pipes was introduced along with the rain inflow. Labonté-Raymond et al. [36] highlighted that climate change has led to a significant escalation in the intensity of extreme rainfalls in Abitibi-Témiscamingue in a way that a single-day rainfall of 77.8 mm in September 2018, surpassed the previously anticipated 100-year recurrence level. The final 3 models (models 13–15) were initially simulated using the average rainfall rate as well as the inlet flow from pipes until reaching a steady state and were then subjected to a 24-h period of 78 mm rainfall along with the inflow from pipes.

Fig. 3 shows all implemented boundary conditions. Low pressure distribution systems were considered and a uniform inflow through the upper half of the perforated pipes was implemented (further explained in the SI, Section 4). The inlet velocities were defined as:

$$\boldsymbol{n_v} \bullet \boldsymbol{u_{2D}} = \frac{Q_{inf}}{86400 L_{1_{2D}} L_{2_{2D}}} \tag{4}$$

where $\boldsymbol{n_v}$ is the outward normal vector, $\boldsymbol{u_{2D}}$ [m/s] and $\boldsymbol{u_{3D}}$ [m/s] are the 2D and 3D inlet velocities, Q_{inf} [m^3/d] is the influent discharge, $L_{1_{2D}}$ [m] is half of the perimeter of all pipes in the 2D cross-section, $L_{2_{2D}}$ [m] is the length of the polishing bed and L^2_{3D} [m^2] is the lateral surface area of the upper half of perforated pipes in the 3D model. 86,400 is the conversion factor.

The water depth in the ditch was set to 15 cm. Hydrostatic pressure was imposed to the boundaries below the water level. A mixed boundary condition was assigned to the boundaries above the water table as:

$$\boldsymbol{n_v} \bullet \boldsymbol{u} = I + R_b(H_b - H) \tag{5}$$

where $\boldsymbol{u}$ [m/s] is the Darcy velocity, I [m/s] is the infiltration rate, R_b [s^{-1}] is the external resistance, H_b [m] is the total external head and H [m] is the total internal head at the boundary.

When the pressure is negative, the mixed boundary switches to $I =$ rainfall rate and $R_b = 0$. As the water table in the sand layer rises above the water level in the ditch, a seepage boundary forms where the saturated porous medium faces the air. An outward flux from the porous media to the ditch occurs through this boundary. In this situation, $I = 0$ and R_b must be large enough to ensure that the boundary's pressure closely approximates atmospheric pressure [37].

It was assumed that rainfall completely infiltrates into the sand layer. However, lowly permeable sediments and topsoil can limit infiltration and entail runoff. To properly model the interaction of surface water and infiltration, a thin runoff layer was considered at the top of the sediments and topsoil. This layer serves as a transitional zone where rainfall can partially infiltrate while also allowing for surface runoff. The idea of incorporating a runoff layer into subsurface modelling was previously introduced and implemented (e.g., [38,39]). Details regarding the selection of the remaining no-flow boundaries are provided in the SI, Section 8.

An inlet P concentration of 5 mg/L was considered. This value is within the range of 3–7 mg P/L which was previously reported for secondary effluent [40]. The initial P concentration within the polishing bed was established at zero.

2.5.2. Governing equations and parameters

Finite element-based software, COMSOL Multiphysics [41] was utilized for numerical simulations. Meshing used in the models and grid

convergence are described in the SI, Section 9. The "Richards' equation" interface was used to model flow in variably saturated soil layers:

$$\frac{\partial\theta}{\partial t}+\nabla\bullet(\boldsymbol{u})=Q \tag{6}$$

where θ [−] is the volumetric water content, $\boldsymbol{u}$ [m/s] is the Darcy velocity, and Q [s^{-1}] is a source/sink term. The Darcy velocity is defined as:

$$\boldsymbol{u}=-K_{sat}k_r\nabla(H_p+z) \tag{7}$$

where K_{sat} [m/s] is the saturated hydraulic conductivity, k_r [−] is the relative permeability, H_P [m] is the pressure head, and z [m] is the vertical coordinate. All soil layers were assumed to be homogenous and isotropic. The pressure head was addressed according to the water content [42]:

$$S_e=\begin{cases}\left(1+\left|\alpha H_p\right|^n\right)^{-m}H_p<0\\ 1\;H_p\geq 0\end{cases}$$

$$\theta=S_e(\theta_s-\theta_r)+\theta_r$$

$$m=1-\frac{1}{n} \tag{8}$$

where S_e [−] is the effective saturation, θ_r [−] is the residual water content, θ_s [−] is the saturated water content which equals porosity, and α [m^{-1}], n [−] and m [−] are van Genuchten parameters. Relative permeability was defined as:

$$k_r=S_e^{0.5}\left(1-\left(1-S_e^{-m}\right)^m\right)^2 \tag{9}$$

The hydraulic properties of the runoff layer were modeled using Richard's equation according to Chapuis [38]. In this layer, the relative permeability was set to 1, and the water content drops from 0.99 to 0.01 as the pore water pressure decreases from 0 to −1 Pa.

Porous media parameters were implemented as presented in Table 2. Further justifications are provided in Section 10 of the SI.

The "Transport of diluted species in porous media" interface was used to model the transport of wastewater P content by the advection-dispersion equation:

$$\frac{\partial(\theta c)}{\partial t}+\frac{\partial(\rho_b c_a)}{\partial t}-\nabla\bullet((D_d+D_e)\nabla c)+\boldsymbol{u}\bullet\nabla c=Q_c \tag{10}$$

where ρ_b [kg/m^3] is the dry bulk density of the soil, D_d [m^2/s] is the dispersion tensor, D_e [m^2/s] is the molecular diffusion constant, and Q_c [$g/m^3/s$] is the source/sink term. Longitudinal and transverse dispersivities and molecular diffusion constant were set to 0.01 m, 0.001 m and 1×10^{-9} m^2/s respectively. Langmuir adsorption isotherm was considered for modelling since it provides the maximum adsorption capacity, which is useful for analysis.

Soil bulk density was calculated as:

$$\rho_b=2650(1-\varepsilon) \tag{11}$$

where 2650 [kg/m^3] is a common value for soil particle density and ε [−] is the porosity.

Soils with larger particles have smaller specific areas and lower adsorption capacities [43]. Therefore, no adsorption capacity was attributed to crushed stone. The adsorption capacity of sand was defined based on experimental results. The impermeable sediment layer is expected to impede the infiltration of flow. As such, the adsorption capacity of sediments is unlikely to change the P removal pattern. For ease of convergence, a uniform adsorption capacity was assigned to sand and sediments.

The two mentioned interfaces were coupled to simulate wastewater transport through STU. Such an approach was successfully applied by Samsó et al. [53].

2.5.3. Output variables

The following variables were calculated using the COMSOL Multiphysics post-processing tools:

- The inlet and outlet P load [g/day] was calculated as the total P flux that enters the polishing bed from the pipes and enters the ditch from the polishing bed, respectively. The 2D fluxes were multiplied by the length of the polishing beds to give comparable values.
- The average outlet P concentration [mg/L] in the outlet flux from the polishing bed to the ditch (at the seepage face boundary) was calculated.
- The lifetime of polishing beds was defined as the duration by which the outlet P load reached 80 % of the inlet P load.

3. Results

3.1. Field inspections: performance of septic systems with borrow sand-based polishing beds

Ground surface flooding, indicative of hydraulic failure, was observed solely in 2 systems out of the 26 studied septic systems. One possible factor could be that, unlike other systems, in one system, the bottom of the ditch is positioned at the same level as the bottom of the sand layer. Since the underlying sediments impede infiltration, this causes the sand layer to be flush with the accumulated water in the ditch, thereby increasing the likelihood of flooding. Additionally, the extended operational duration of the other system (installed in 2012) could also play a role in the observed outcome.

Nine properties had ditches without enough water for sampling. This could result from low wastewater production from households or deeper effluent percolation in some settings. Total P concentrations measured in water from the ditches of the rest of the septic systems are shown in Fig. 4. Bars show the average values and error bars show the maximum and minimum data. In septic systems 1–12, water was present all through the ditches while in systems 13–17, water was only present downstream of the polishing beds. Nine systems out of the first 12 systems showed an increase in P concentration at the outlet of septic systems. Table 3 shows the released P from septic systems 1–12. The released P was >9 mg/L in systems 1–3, >1 mg/L in systems 4–7, but <1 mg/L in systems 8 and 9.

To prevent eutrophication, the U.S. Environmental Protection Agency (EPA) has established guidelines that limit total P in flowing waters to a maximum of 0.1 mg/L [44]. In addition, Québec's environmental standards set a threshold of 0.03 mg/L for total P in surface waters [45]. In the current study, all ditch samples contained P

Table 2
Porous media parameters used for modelling.

	Hydraulic conductivity K_{sat} [m/s]	Porosity ε [–]	Residual water content θ_r [–]	van-Genuchten parameter α [m^{-1}]	van-Genuchten parameter n [–]
Topsoil	3×10^{-6}	0.52	0.15	2.42	1.46
Sand	4.5×10^{-3}	0.39	0.03	12.00	2.50
Fine sediment	6×10^{-8}	0.54	0.26	4.53	1.51
Crushed stone	2.5	0.52	0	20.00	2.20
Runoff layer	45	1	0	–	–

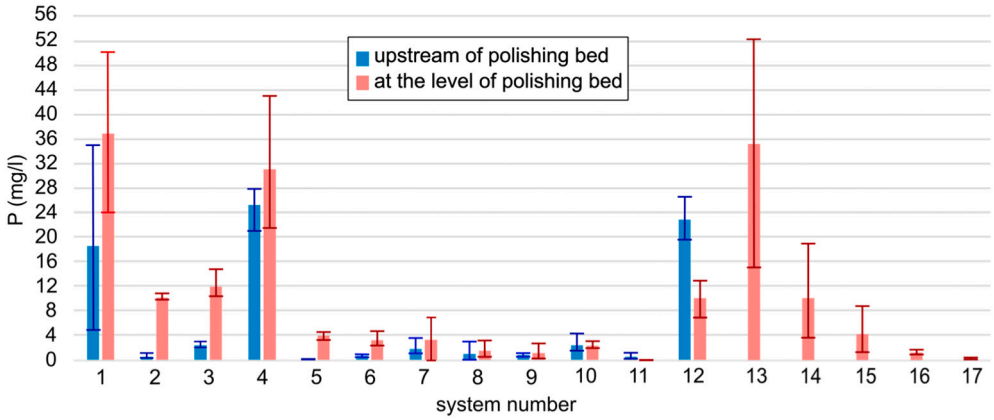

Fig. 4. P concentration upstream and at the level of the polishing beds in ditches.

Table 3
P released from septic systems.

System number	P released from septic system (mg/L)	System number	P released from septic system (mg/L)
1	18.29	7	1.49
2	9.59	8	0.50
3	9.47	9	0.32
4	5.86	10	−0.06
5	3.88	11	−0.55
6	2.53	12	−12.79

concentrations equal to or exceeding the 0.03 mg/L threshold. Furthermore, the observed P releases in the ditches, reaching up to 18.29 mg/L, underscores a significant P discharge that could potentially lead to adverse environmental impacts.

In systems 10–12, the P concentration at the level of the polishing bed was smaller than the upstream concentration (negative values of released P). This could be due to P uptake by plants and microbes, presence of other sources of contamination, complex flow in the ditches, or the dilution of effluent at the outlet with any sort of uncontaminated water (e.g., rain water).

Sanitary inspections included diverse polishing beds from the three main categories, installed between 2009 and 2020, with both gravity-fed and low-pressure systems, 1 to 6 bedrooms, and varying occupation rates. Differences in P removal performance can stem from the abovementioned properties and other factors such as P inlet from the household and the properties of the borrow sand. The average installation year of all 17 systems is 2015. Even relatively young systems such as systems 2 and 4, installed in 2018, show high P releases. Overall, sanitary inspections indicated that the targeted septic systems have significant potential for releasing P into the environment, as evidenced by the increase in P concentration at the level of the majority of polishing beds.

3.2. Characterization of native soil; particle distribution and permeability

The clay content exceeded 64 % in 15 samples, with 4 samples ranging between 33 % and 45 %. Only one sample exhibited a clay content below 25 %. Detailed particle distribution of the samples is presented in the SI, Section 11. Since the target area is located within the Clay Belt, the general clayey nature of the region is well known. Still, this quantitative data further characterized the site-specific soil properties critical for the design and performance evaluation of STUs. Despite this variability, all samples were classified as impermeable. The impermeability of this natural environment hinders infiltration, making the installation of SUTs with the natural soil impractical. Consequently, there is a need to utilize borrow sand for the construction of STUs. This is consistent with municipal records, indicating that many septic systems in the area have been constructed with borrow sand in impermeable soil.

3.3. Sand phosphorus adsorption isotherms

Freundlich and Langmuir isotherms parameters are reported in Table 4. Overall, both isotherms fitted well ($R^2 > 0.84$), although Freundlich isotherm provided a better fit for S1 ($R^2 > 0.94$). Fig. 5 shows the experimental data and fitted isotherms.

S1 has a greater sorption capacity compared to S2. The reason might be that S1 is more poorly sorted and contains more fines with greater surface areas for adsorption (Particle distribution curves in Fig. S3 of the SI). Additionally, pH measurements (pH values are detailed in the SI, Section 12) suggest that the mineral composition of the sands plays a role in adsorption efficiency. The initial solution pH ranged from 5.4 to 5.8, indicating slightly acidic conditions. After agitation, the pH of S2 samples remained in the acidic range (4.8–5.0), whereas S1 samples shifted to a near-neutral to slightly alkaline range (6.8–7.1). This difference suggests that S1 contains minerals capable of neutralizing acidity, whereas S2 lacks sufficient buffering capacity, maintaining an acidic environment.

Previous studies indicate that the optimal pH range for phosphorus adsorption is 5–7 [46]. While the initial solution pH was within this range, the post-agitation pH of S2 samples dropped below the optimal range, potentially reducing its adsorption efficiency. This highlights the importance of mineral composition and pH buffering in phosphorus retention, further explaining the superior adsorption performance of S1.

3.4. Numerical simulation of polishing beds

In 2D simulations of models 1–12, following a steady-state saturation condition established with rain inflow, the water table reached stability within 100 days upon introducing inflow from pipes in addition to the rainfall inflow. This suggests a balance between water inflow, outflow, and storage within the system. Notably, our study employed an average rainfall rate. However, it is important to acknowledge that in reality, seasonal variations lead to fluctuations in the water table.

Fig. 6 shows the steady-state water tables for day 360 or 180. In all

Table 4
Freundlich and Langmuir isotherm parameters for S1 and S2.

	Freundlich isotherm			Langmuir isotherm		
	k_F $\left[(g/kg)\ (mg/L)^{-b_F}\right]$	b_F [–]	R^2	k_L [mg/kg]	b_L [mg/L]$^{-1}$	R^2
S1	6.627×10^{-3}	0.737	0.947	88.49	0.072	0.848
S2	6.715×10^{-3}	0.265	0.953	17.12	0.318	0.957

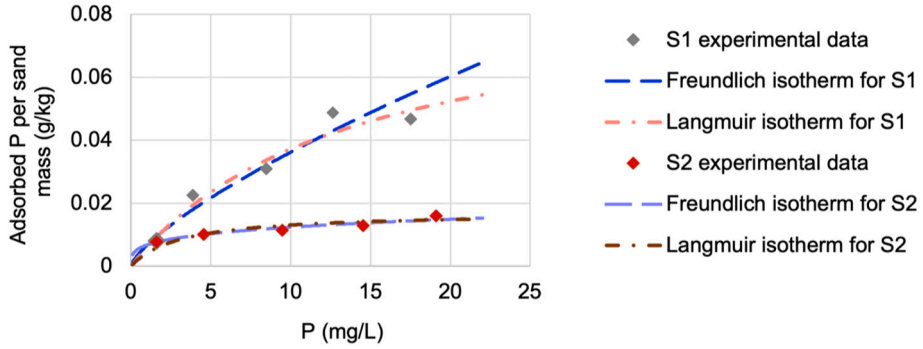

Fig. 5. Adsorption experimental data and Freundlich and Langmuir isotherms for S1 and S2.

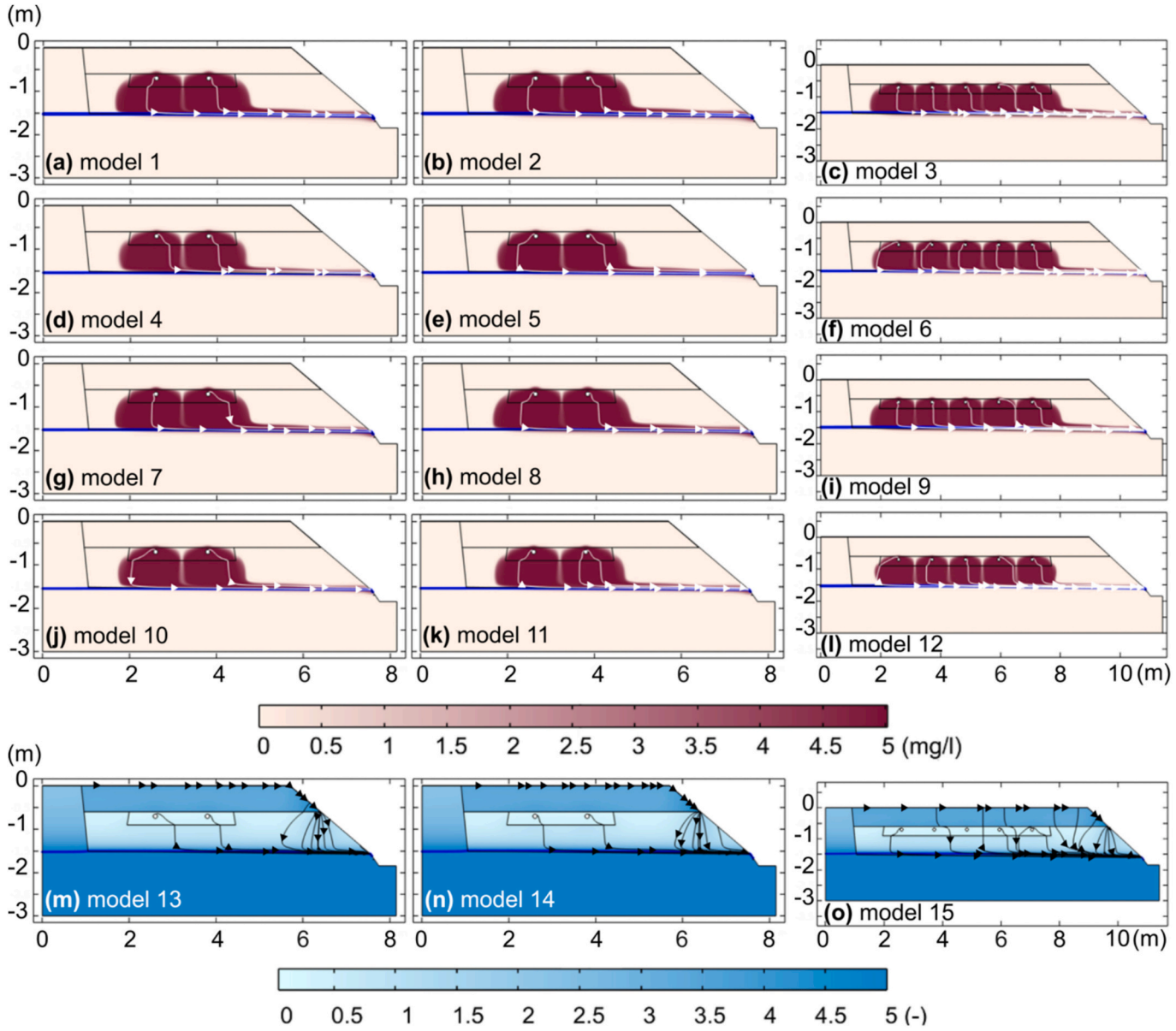

Fig. 6. 2D contour maps of P concentration, water table (blue line), and streamlines, (a–f) models 1–6 in day 360, (g–l) models 7–12 in day 180. 2D contours of saturation degree and streamlines, (m–o) models 12–15 after 24 h of heavy rain. (For interpretation of the references to colour in this figure legend, the reader is referred to the web version of this article.)

Table 5
Minimum unsaturated depths for models 1–15 and lifetimes for models 1–12.

Model number	Minimum unsaturated depth below crushed stone [m]	Lifetime [days]
1	0.60	110
2	0.59	85
3	0.56	68
4	0.62	243
5	0.61	180
6	0.60	145
7	0.60	50
8	0.59	39
9	0.56	30
10	0.62	99
11	0.61	78
12	0.60	67
13	0.58	
14	0.58	
15	0.55	

models, a seepage boundary face was established, extending from the water level in the ditch to a few centimeters above the sediment layers. The steady-state minimum unsaturated thicknesses below the crushed stone layer are presented in Table 5. Being designed for 6-bedroom buildings, models 2 and 3 show the lowest minimum unsaturated thicknesses among models 1–6. The average minimum unsaturated thicknesses in models 4–6 were greater than models 1–3, due to smaller influent discharge from the pipes. Models 7–12 are hydraulically identical to models 1–6. Maintaining the appropriate unsaturated thicknesses in the polishing bed is crucial to ensuring the sufficient oxygen levels required to support aerobic microorganisms and oxidation reactions. Here, the highly permeable sand layer was conductive to the efficient movement of water toward the ditch without a considerable water table rise. Given that the minimum thickness of the sand layer below the crushed-stone layer is 0.6 m (Fig. 3), the sand layer remained mostly unsaturated. This finding is corroborated by field observations of rare flooding events and suggests the reliability of the models in predicting the hydraulic performance of the systems.

Fig. 6m, n and o and the minimum unsaturated thicknesses of models 13–15 (Table 5) reveal that even during harsh rain events, the sand layer remained mostly unsaturated. The streamlines in Fig. 6m, n and o showed that the infiltrating rainfall reaches the highly permeable sand layer and flows toward the ditch.

Fig. 7a and b displays the inlet and outlet P loads in models 1–12 and the lifetimes of polishing beds are reported in Table 5. Models 1–6 and 7–12 had approached P adsorption saturation by day 360 and 180, respectively. As shown in Fig. 5, the P plume in all models at the time of saturation occupied the part of sand below the crushed stone as well as small minor parts above sediments toward the ditch. The evolution of P plume with time was further discussed in the SI, section 13.

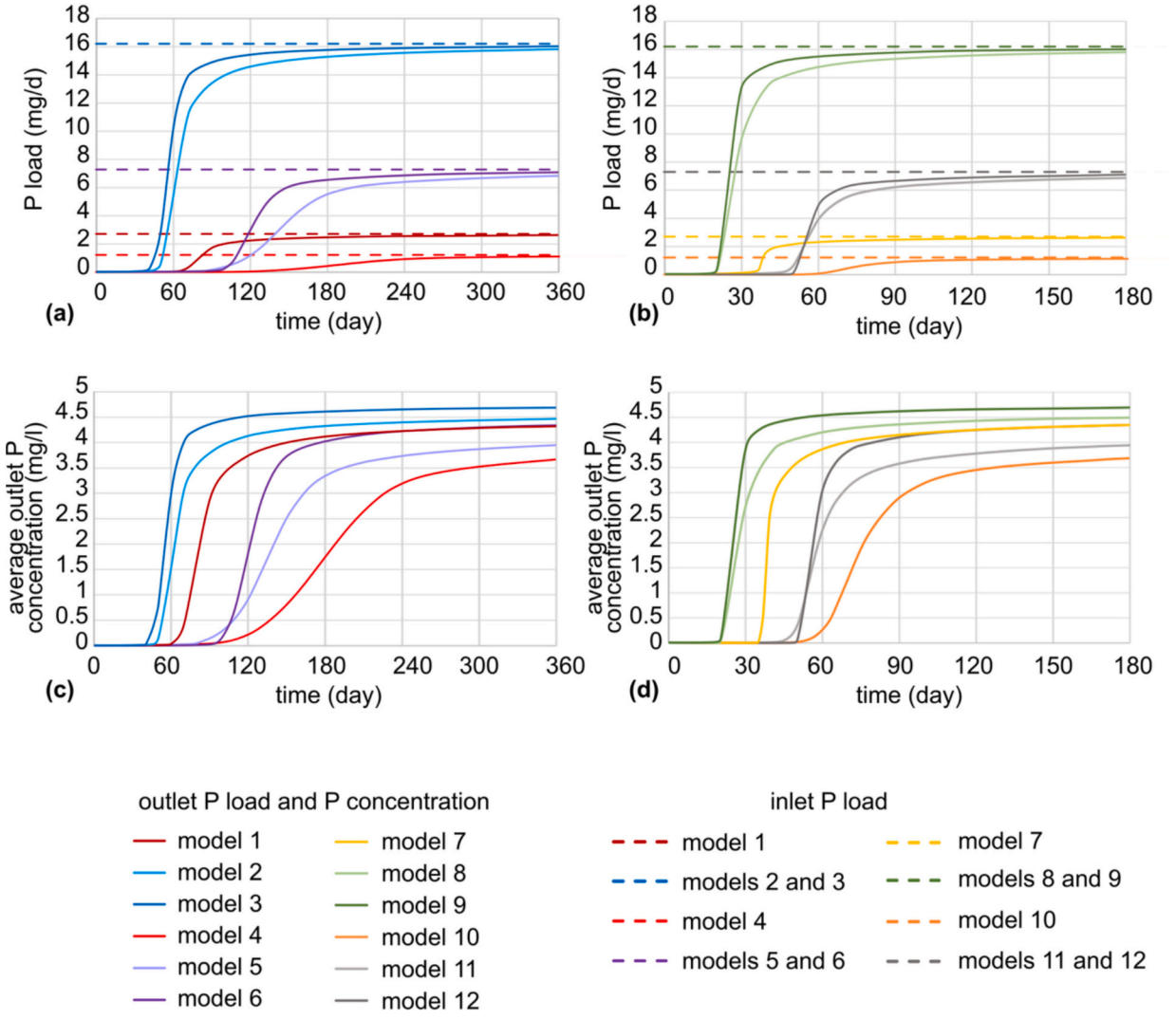

Fig. 7. Inlet and outlet P load for (a) models 1–6 and (b) models 7–12. Average outlet P concentration for (c) models 1–6 and (d) models 7–12.

Overall, numerical simulations suggests that all studied polishing beds have short P-sorption lifetimes, specifically less than a year. The implication is that systems operating beyond this timeframe would lead to reduced removal effectiveness and subsequent environmental releases. Moreover, the results of sanitary inspections of the studied STUs, revealing systematic phosphorus release from systems aged 2 to 17 years, confirm the trend of P release from systems. Therefore, the reliability of the models is supported by their consistency with real-world data, reinforcing their validity for understanding P dynamics in these systems. The findings of numerical modelling explain the potential reasons behind the release of P, as observed in the field inspections.

The influent quantity and the sand available for P sorption led to variations in the calculated STU lifetimes. On average, the lifetimes of systems designed for 1 bedroom were 44 % longer than those designed for 6 bedrooms. Rectangular beds and square beds have equivalent actual discharges and bed areas (surface area of the crushed stone layer). However, in comparison to square polishing beds, rectangular ones have greater bed lengths with identical distances from the edge of the crushed stone to the ditch (polishing beds' plans in Fig. S4 of the SI) which gives more available sand beside the actual polishing bed. Consequently, rectangular polishing beds had 24 % longer average lifetimes compared to square beds. The lifetimes of polishing beds performing at a 45 % occupancy rate were on average 110 % longer than those designed for full occupancy. Furthermore, the lifetimes of polishing beds constructed with S1 were 130 % longer than polishing beds constructed with S2.

According to Fig. 7c and d, the average outlet P concentration never quite reached the inlet P concentration of 5 mg/L despite increasing to reach close values. Within the same timeframe, the outlet P load almost matched the inlet P load. This outcome is the result of accounting for a dilution by a rainwater inlet discharge in addition to the inlet discharge from the pipes. While the rainwater did not change the total inlet and outlet P load, it diminished the P concentration in the outlet flux.

A mass balance approach quantifies the impact of rainfall-induced dilution on P concentrations. Assuming complete mixing of effluent from the polishing bed (p) and rainwater (r) in the downgradient ditch, the mass balance equation is expressed as: $c_pQ_p + c_rQ_r = c_tQ_t$ where c represents P concentration, Q represents discharge, and t refers to the mixture in the ditch. Given that rainwater does not contain P ($c_r = 0$), the equation simplifies to $c_t = \frac{C_p}{\left(1+\frac{Q_r}{Q_p}\right)}$. Here, $1 + \frac{Q_r}{Q_p}$ represents the dilution factor, indicating the extent to which rainfall influences P concentrations in the ditch. Therefore, greater ratios of the rainwater discharge to the polishing beds' discharge led to lower outlet concentrations. Consequently, models designed for single bedroom and models operating with occupancy-dependent actual discharges yielded lower final P concentrations. The total surface area exposed to rain is greater in rectangular beds than in square beds leading to rectangular polishing beds experiencing lower final outlet P concentrations. Finally, systems with S2 reached higher P outlet concentrations earlier than systems with S1 due to differences in sorption capacities. However, since the sorption capacity of sand isn't tied to discharges, it is not effective in the final outlet P concentrations.

Setting a threshold where rainfall-induced dilution is considered negligible, defined as $c_t > 0.9c_p$, results in $\frac{Q_p}{9} > Q_r$. For example, in model 1, where $Q_p = 0.54$ m^3/d, this condition leads to $Q_r < 0.06$ m^3/d. Assuming that rainfall on the surface area shown in Fig. 3a (length = 2.92 m and total width = 7.55 m) contributes to the ditch, with a surface area of 22 m^2, this corresponds to a rainfall intensity of 2.72 mm/day. This value is slightly higher than the average rainfall of 2.5 mm/day in the region [36], suggesting that typical rainfall events may have a limited impact on dilution. However, assuming the same surface area and a torrential rainfall of 78 mm/day leads to $c_t = 0.24c_p$ indicating that extreme precipitation can significantly reduce P concentrations. Since the study area experiences dry summers [36], rainfall-induced dilution is expected to be negligible during those periods but should not be overlooked in wet seasons, where it may play a crucial role in reducing P concentrations in the receiving environment.

4. Discussions

4.1. Key factors in the design of borrow sand-based STUs

Given the impermeability of the native soil in the target site, Abitibi-Témiscamingue, and the considerable hydraulic loads (higher than those typically applied to drain fields) imposed to the polishing beds, the native soil could not be used for efficient infiltration. As a result, the design of the outlet for the discharge from the STUs and its connection to surface water played a critical role in maintaining hydraulic performance and preventing flooding. Our system utilized a drainage ditch as the outlet, a design confirmed through numerical simulations to be effective under applied hydraulic loads (0.03 to 0.10 m/d) and rainfall of 2.5 mm/d.

Simulations further demonstrated that the implemented outlet design efficiently managed extreme rainfall conditions. During a modeled event with 78 mm/d of rainfall, the sand layer effectively directed water toward the ditch, maintaining unsaturated conditions and preventing waterlogging. This confirms that systems with well-designed drainage ditches offer a robust solution in impermeable settings, whereas designs relying on natural infiltration or piped outlets to surface water, as reported in previous studies (e.g., [5,20]), may not perform as effectively under similar conditions with highly impermeable natural beds.

Two sands were selected based on availability and local regulations to reflect the materials likely used in STUs' installations. Maximum Langmuir adsorption capacities obtained from batch tests were 17.1 and 88.5 mg P/kg, aligning with previously reported values for sands used in other wastewater systems. For example, Florida and Danish sands reported ranges of 14 to 270 mg P/kg [15,47]. In a literature review of previous studies, McCray et al. [14] reported an average maximum P sorption capacity of 40 mg/kg (n = 12) for sand which aligns with the capacities observed in this study. In general, natural soils with coarse grains generally show low P adsorption capacities (<100 mg/kg); while other materials such as fly ash and red mud show higher adsorption capacities (>10 g/kg) [48].

The simulations revealed that the adsorption capacity of the sands was exhausted within less than a year, which corresponds with the P release observed during field inspections. In addition to adsorption capacity, other factors such as sand thickness also significantly influenced performance. The available sand thickness in this study was 0.6 m, whereas other borrow-sand-based STUs reported greater depths, such as 1 to 2 m in the study by Robertson et al. [18] and over 0.8 m in the study by Eveborn et al. [20].

Hydraulic loading rates are similarly crucial to P removal since it directly affect the input P to the system. The inspected systems operated with loads ranging from 0.025 to 0.077 m/d. Numerical simulations explored scenarios with 0.034 and 0.045 m/d based on a 45 % occupancy rate and models simulated under full design capacity included hydraulic loads between 0.077 and 0.101 m/d. Previously, Robertson et al. [18] observed successful P retention in borrow sand STUs under low hydraulic loads (<0.02 m/d). In contrast, Eveborn et al. [20] documented performance challenges at higher loads (up to 0.33 m/d), suggesting that the hydraulic loading rate could have contributed to the observed differences in system performance.

4.2. Recommendations for future system design and maintenance

To enhance P retention potential of future STUs, we recommend increasing the polishing bed size, both in depth and area. This approach provides more media available for P sorption and would extend the lifespan of P sorption. A sand thickness of at least 1.0 m and a hydraulic

load limit of <0.03 m/d would provide improved long-term performance.

For the construction of future systems, pre-installation adsorption tests on potential borrow sands are recommended to estimate maximum sorption capacities. The choice of adsorbent should consider factors beyond availability and regulatory compliance, including the ability to maintain long-term performance, sustainability and environmental impact. In the context of this study, since the native soil is impermeable, the permeability of the filter material should be high enough. For instance, Cucarella & Renman [48] categorized fly ash and red mud with high P adsorption capacities (>10 g P/kg). However, their fine particle size (<0.15 mm) can cause hydraulic issues, making them unsuitable for the targeted systems of this study. While sands support hydraulic performance, which is essential for target systems in this study, their ability to retain P is not always efficient. It is recommended to use materials with capacities above 100 mg P/kg. If local sands fail to meet these criteria, incorporating P-sorbing alternatives and amendments should be considered.

As noted by McCray et al. [14], some sands can achieve P adsorption capacities up to 1.3 g P/kg, which could be implemented in future systems to enhance P removal. Additionally, other natural materials, such as marine sediments, are rich in calcium and magnesium carbonates and have a high specific surface and a high porosity, which make them suitable candidates for P removal in wastewater treatment systems [49]. Shell sands have been reported to have P adsorption capacities of 14–17 g P/kg [50]. Another alternative is biochar, which can be produced from various organic waste materials, promoting sustainability and contributing to waste reuse. Iron- and calcium-impregnated biochar has been shown to achieve a P adsorption capacity of up to 3.21 g P/kg and can be used as an amendment layer to improve filter media in terms of P adsorption as demonstrated by Dalahmeh et al. [51]. Biochar's large surface area, high porosity, and ability to retain P make it a viable option for improving P retention and maintaining hydraulic performance.

Monitoring strategies are critical for early detection of system failures. Routine measurements at outlet ditches should be conducted to identify potential issues. Given that rainfall can dilute the effluent, as demonstrated by our numerical simulations, we recommend measuring both the discharge in the ditches and the P concentration to calculate P loads (P mass per unit time) rather than relying solely on concentration measurements. This approach is particularly important during wet seasons, where relying solely on concentration measurements may underestimate actual P transport. It is important to note that very few field studies accounted for dilution correction when estimating P removal [17]. When early signs of P release are detected, maintenance actions should be undertaken promptly to prevent environmental impacts. Maintenance could include partial or complete replacement of the sand layer with virgin sand or the addition of P-sorbing amendments to enhance retention capacity.

In impermeable settings, proper outlet design, is essential to prevent waterlogging and maintain unsaturated conditions in the sand layer. Field inspections revealed that while most systems performed well, one case of flooding occurred due to improper ditch configuration. In this case, the bottom of the ditch was level with the sand layer, causing water to accumulate. Therefore, for future constructions, it is recommended that the ditch be positioned lower than the sand layer to prevent water accumulation and ensure effective drainage. Maintaining a stable water level in the ditch below the sand layer is also critical, as excessive water levels can lead to saturation and reduced system performance. To achieve this, it is recommended to build ditches with a slope along their length. This way, continuous flow away from the system could be achieved. Additionally, a slope at the bottom of the sand layer is necessary to direct infiltrated water toward the ditch efficiently. For example, in the studied cross-section (Fig. 3b and d), a 1 % slope was implemented to facilitate proper drainage and prevent water stagnation within the sand layer. These strategies can be broadly applied to the design and construction of borrow sand-based STUs in impermeable settings to enhance drainage efficiency and prevent hydraulic failures.

After construction, visual inspections of drainage ditches and regular monitoring of water levels in drainage ditches are crucial. While it is recommended to avoid P inspections immediately after extreme rainfall events due to the potential underestimation of released P, it is advised to inspect systems for hydraulic performance during significant rainfall events. Signs of flooding or a sharp rise in water levels may indicate hydraulic performance issues. In such cases, deepening the ditch to make sure that the STU does not get flush with water in the ditch should be a priority.

Thoughtful outlet design and routine maintenance involve relatively low costs compared to the potential expense of system failures. While P-sorbing amendments or supplementary treatments may incur additional costs, their long-term benefits (such as reduced maintenance frequency and improved P retention) justify the investment. By implementing these strategies, STUs can be designed to achieve sustainable wastewater management in impermeable environments, safeguarding both groundwater and surface water quality.

5. Conclusions

This study provides a novel contribution to the understanding and optimization of borrow sand-based STUs in impermeable settings. Unlike STUs in naturally permeable soils, where deeper layers contribute to P removal and hydraulic performance, borrow sand-based systems depend entirely on the finite adsorption capacity of the sand layer and require carefully designed connections to surface water to prevent waterlogging. By integrating field inspections, experimental analyses, and numerical modelling, this study uniquely combines real-world observations with predictive tools to evaluate the dual challenges of hydraulic performance and P retention. Moreover, by addressing both hydraulic and hydrogeochemical challenges, this work provides a transferable framework for optimizing decentralized wastewater treatment systems in impermeable settings. The borrow sand-based polishing beds within the impermeable and clay-rich natural covering of Abitibi-Témiscamingue served as a case study. The following conclusions were drawn:

- Flooding, a common indicator of hydraulic failure, was rarely observed in polishing beds with proper designs that direct effluent toward drainage ditches. The sand layer in polishing beds remains mostly unsaturated even during extreme rainfall events.
- The sands used in this study, selected for availability and regulatory compliance, showed Langmuir adsorption capacities of <100 mg P/kg, aligning with values reported for natural soils with coarse grains.
- Relatively high P background concentrations were detected in the ditches downgradient from the septic systems. Still, a systematic release of P (up to 18.29 mg/L) caused by septic systems was detected.
- Insufficient sorption capacity of the borrow sands leads to systems getting saturated with P in less than a year. Early polishing beds' P saturation resulted in considerable P release from septic systems, rendering them ineffective for P removal.
- The findings suggest that current STU designs are ineffective for long-term P removal, necessitating design improvements and alternative materials with higher P sorption capacities.
- Rainfall can diminish the concentration of contaminants in the effluent of septic systems. It is crucial to monitor mass loads instead of relying on concentrations to avoid overrating systems' performances.
- 2D models are suitable for the successful modelling of hydraulic integrity in a sloped STU. Unlike 3D models, 2D models do not consider contaminants dispersion perpendicular to the STU slope. Nevertheless, this discrepancy does not lead to a systematic and significant difference.

This study is believed to shed light on the effectiveness of borrow-sand STUs within septic systems, provide critical insights for policy-makers and researchers, and contribute to the development of sustainable wastewater treatment practices that safeguard both surface water and groundwater quality in challenging settings. Future work should focus on long-term monitoring of P desorption risks, the influence of bio-clogging and seasonal dynamics, the role of growing vegetation, and further refinement of outlet designs such as drainage ditches.

CRediT authorship contribution statement

Sorour Sheibani: Writing – review & editing, Writing – original draft, Software, Methodology, Investigation, Formal analysis, Conceptualization. **Michelle Nasrallah:** Writing – review & editing, Methodology, Formal analysis. **Benoît Courcelles:** Writing – review & editing, Supervision. **Eric Rosa:** Writing – review & editing, Conceptualization. **Brahim Maylal:** Writing – review & editing, Methodology. **Dominique Claveau-Mallet:** Writing – review & editing, Supervision, Project administration, Funding acquisition, Conceptualization.

Declaration of competing interest

The authors declare that they have no known competing financial interests or personal relationships that could have appeared to influence the work reported in this paper.

Acknowledgements

The authors thank Polytechnique Montreal technicians Samuel Chénier and Éric Turgeon for their help in soil characterization experiments and Mélanie Bolduc and Gabriel St-Jean for their help in phosphorus adsorption tests. We extend our gratitude to OBVAJ (Organisme de bassin versant Abitibi-Jamésie*)* for their effort in field inspections and data collection. We would also like to thank MELCCFP (Ministère de l'Environnement, de la Lutte contre les changements climatiques, de la Faune et des Parcs) for providing municipal documents and Patrick Morin for his effort in documenting municipal records. This project was funded by MELCCFP, the National Science and Engineering Research Council of Canada (grant number ALLRP 570383-21) and the Canada Research Chair in Decentralized and Small-Scale Water Treatment (grant number 950-232871). Sorour Sheibani was supported by Quebec Research Fund - Nature and Technologies (FRQNT) doctoral awards (B2X).

Appendix A. Supplementary data

Supplementary data to this article can be found online at https://doi.org/10.1016/j.jwpe.2025.107681.

Data availability

Some data is confidential. The rest will be made available upon request

References

[1] L.W. Canter, R.C. Knox, Septic Tank System Effects on Ground Water Quality, Routledge, 2017, https://doi.org/10.1201/9780203739877.
[2] M.G. Lusk, G.S. Toor, Y.-Y. Yang, S. Mechtensimer, M. De, T.A. Obreza, A review of the fate and transport of nitrogen, phosphorus, pathogens, and trace organic chemicals in septic systems, Crit. Rev. Environ. Sci. Technol. 47 (7) (2017) 455–541, https://doi.org/10.1080/10643389.2017.1327787.
[3] Government of Canada, About Your House, Your Septic System, Canada Mortgage and Housing Corporation, 2001. https://publications.gc.ca/collections/collection_2011/schl-cmhc/nh18-24/NH18-24-34-2008-eng.pdf.
[4] S. Luanmanee, T. Attanandana, T. Masunaga, T. Wakatsuki, The efficiency of a multi-soil-layering system on domestic wastewater treatment during the ninth and tenth years of operation, Ecol. Eng. 18 (2) (2001) 185–199, https://doi.org/10.1016/S0925-8574(01)00077-5.
[5] J.C. Converse, E.J. Tyler, Wisconsin mound performance, Small Scale Waste Manage. Proj. 345 (1986).
[6] Ministry of Environment and Climate Change, On-site sewage disposal systems standard. https://novascotia.ca/nse/wastewater/docs/On-Site-Sewage-standard-June-2022.pdf, 2022.
[7] P. Havard, R. Jamieson, D. Cudmore, L. Boutilier, R. Gordon, Performance and hydraulics of lateral flow sand filters for on-site wastewater treatment, J. Hydrol. Eng. 13 (8) (2008) 720–728, https://doi.org/10.1061/(ASCE)1084-0699(2008)13:8(720).
[8] Intergovernmental Panel on Climate Change, Climate Change 2021: The Physical Science Basis. Contribution of Working Group I to the Sixth Assessment Report of the Intergovernmental Panel on Climate Change (Chapter 11: Weather and Climate Extreme Events in a Changing Climate), 2021.
[9] R.A. Smith, R.B. Alexander, G.E. Schwarz, Natural background concentrations of nutrients in streams and rivers of the conterminous United States, Environ. Sci. Technol. 37 (14) (2003) 3039–3047, https://doi.org/10.1021/es020663b.
[10] M.J. Bowes, C. Neal, H.P. Jarvie, J.T. Smith, H.N. Davies, Predicting phosphorus concentrations in British rivers resulting from the introduction of improved phosphorus removal from sewage effluent, Sci. Total Environ. 408 (19) (2010) 4239–4250, https://doi.org/10.1016/j.scitotenv.2010.05.016.
[11] A.C. Edwards, P.J.A. Withers, Transport and delivery of suspended solids, nitrogen and phosphorus from various sources to freshwaters in the UK, J. Hydrol. 350 (3–4) (2008) 144–153, https://doi.org/10.1016/j.jhydrol.2007.10.053.
[12] K.S. Lowe, Influent constituent characteristics of the modern waste stream from single sources, Water Intell. Online 9 (2010), https://doi.org/10.2166/9781780403519.
[13] M. Lusk, G.S. Toor, T. Obreza, Onsite sewage treatment and disposal systems: phosphorus, EDIS 2011 (8) (2011), https://doi.org/10.32473/edis-ss551-2011.
[14] J.E. McCray, S.L. Kirkland, R.L. Siegrist, G.D. Thyne, Model parameters for simulating fate and transport of on-site wastewater nutrients, Ground Water 43 (4) (2005) 628–639, https://doi.org/10.1111/j.1745-6584.2005.0077.x.
[15] M. Del Bubba, C.A. Arias, H. Brix, Phosphorus adsorption maximum of sands for use as media in subsurface flow constructed reed beds as measured by the Langmuir isotherm, Water Res. 37 (14) (2003) 3390–3400, https://doi.org/10.1016/S0043-1354(03)00231-8.
[16] R. Hamisi, A. Renman, G. Renman, A. Wörman, R. Thunvik, Long-term phosphorus sorption and leaching in sand filters for onsite treatment systems, Sci. Total Environ. 833 (2022) 155254, https://doi.org/10.1016/j.scitotenv.2022.155254.
[17] M. Wang, F. Zeng, S. Chen, L.M. Wehrmann, S. Waugh, B.J. Brownawell, C. J. Gobler, X. Mao, Phosphorus attenuation and mobilization in sand filters treating onsite wastewater, Chemosphere 364 (2024) 143042, https://doi.org/10.1016/j.chemosphere.2024.143042.
[18] W.D. Robertson, D.R. Van Stempvoort, S.L. Schiff, Review of phosphorus attenuation in groundwater plumes from 24 septic systems, Sci. Total Environ. 692 (2019) 640–652, https://doi.org/10.1016/j.scitotenv.2019.07.198.
[19] D. Eveborn, D. Kong, J.P. Gustafsson, Wastewater treatment by soil infiltration: long-term phosphorus removal, J. Contam. Hydrol. 140–141 (2012) 24–33, https://doi.org/10.1016/j.jconhyd.2012.08.003.
[20] D. Eveborn, J.P. Gustafsson, E. Elmefors, L. Yu, A.-K. Eriksson, E. Ljung, G. Renman, Phosphorus in soil treatment systems: accumulation and mobility, Water Res. 64 (2014) 42–52, https://doi.org/10.1016/j.watres.2014.06.034.
[21] V. Cloutier, D. Blanchette, P.L. Dallaire, S. Nadeau, É. Rosa, M. Roy, Projet d'acquisition de connaissances sur les eaux souterraines de l'Abitibi-Témiscamingue (partie 1), 2013.
[22] V. Cloutier, É. Rosa, S. Nadeau, P.L. Dallaire, D. Blanchette, M. Roy, Projet d'acquisition de connaissances sur les eaux souterraines de l'Abitibi-Témiscamingue (partie 2), 2015.
[23] V. Cloutier, E. Rosa, M. Roy, S. Nadeau, D. Blanchette, P.L. Dallaire, G. Derrien, J. J. Veillette, Atlas hydrogéologique de l'Abitibi-Témiscamingue, Presses de l'Université du Québec, 2016.
[24] S. Nadeau, E. Rosa, V. Cloutier, Stratigraphic sequence map for groundwater assessment and protection of unconsolidated aquifers: a case example in the Abitibi-Témiscamingue region, Québec, Canada, Can. Water Resour. J./Rev. Can. Ressour. Hydr. 43 (2) (2018) 113–135, https://doi.org/10.1080/07011784.2017.1354722.
[25] S. Nadeau, E. Rosa, V. Cloutier, R.-A. Daigneault, J. Veillette, A GIS-based approach for supporting groundwater protection in eskers: application to sand and gravel extraction activities in Abitibi-Témiscamingue, Quebec, Canada, J. Hydrol. Reg. Stud. 4 (2015) 535–549, https://doi.org/10.1016/j.ejrh.2015.05.015.
[26] MELCCFP, Ministère de l'Environnement, de la Lutte contre les Changements Climatiques, de la Faune et des Parcs, Guide technique sur le traitement des eaux usées des résidences isolées (Partie B). (2015).
[27] MELCCFP, Ministère de l'Environnement, de la Lutte contre les changements climatiques, de la Faune et des Parcs, in: Guide pour l'étude des technologies conventionnelles de traitement des eaux usées d'origine domestique chap. 3, 2017.
[28] MELCCFP, Ministère de l'Environnement, de la Lutte contre les changements climatiques du Québec, Centre d'Expertise en Analyse Environnementale du Québec, Détermination du Phosphore Total dans les Eaux Naturelles par Minéralisation au Persulfate: Méthode Colorimétrique Automatisée et Procédures Adaptées pour le Phosphore de Faible Concentration et à l'État de Trace, 2019.
[29] ASTM International, ASTM C136M, Standard Test Method for Sieve Analysis of Fine and Coarse Aggregates, 2020.
[30] R.A. García-Gaines, S. Frankenstein, USCS and the USDA Soil Classification System: Development of a Mapping Scheme, 2015.
[31] L. Metcalf, H.P. Eddy, G. Tchobanoglous, Wastewater Engineering: Treatment, Disposal, and Reuse vol. 4, McGraw-Hill, 1991.

[32] ASTM International, ASTM D4646-16, Standard Test Method for 24-h Batch-type Measurement of Contaminant Sorption by Soils and Sediments, 2016.
[33] E. Marafini, M. La Rocca, A. Fiori, I. Battiato, P. Prestininzi, Suitability of 2D modelling to evaluate flow properties in 3D porous media, Transp. Porous Media 134 (2) (2020) 315–329, https://doi.org/10.1007/s11242-020-01447-4.
[34] M. Berlin, G.S. Kumar, I.M. Nambi, Numerical modeling on the effect of dissolved oxygen on nitrogen transformation and transport in unsaturated porous system, Environ. Model. Assess. 19 (4) (2014) 283–299, https://doi.org/10.1007/s10666-014-9399-1.
[35] K.T.B. MacQuarrie, E.A. Sudicky, W.D. Robertson, Numerical simulation of a fine-grained denitrification layer for removing septic system nitrate from shallow groundwater, J. Contam. Hydrol. 52 (1–4) (2001) 29–55, https://doi.org/10.1016/S0169-7722(01)00152-8.
[36] P.-L. Labonté-Raymond, T. Pabst, B. Bussière, É. Bresson, Impact of climate change on extreme rainfall events and surface water management at mine waste storage facilities, J. Hydrol. 590 (2020) 125383, https://doi.org/10.1016/j.jhydrol.2020.125383.
[37] T.F.M. Chui, D.L. Freyberg, The use of COMSOL for integrated hydrological modeling, in: Proceedings of the COMSOL Conference, 2007.
[38] R.P. Chapuis, Numerical modeling of reservoirs or pipes in groundwater seepage, Comput. Geotech. 36 (5) (2009) 895–901, https://doi.org/10.1016/j.compgeo.2009.01.005.
[39] S. Weill, E. Mouche, J. Patin, A generalized Richards equation for surface/subsurface flow modelling, J. Hydrol. 366 (1–4) (2009) 9–20, https://doi.org/10.1016/j.jhydrol.2008.12.007.
[40] R.J. Banu, K.U. Do, I.T. Yeom, Phosphorus removal in low alkalinity secondary effluent using alum, Int. J. Environ. Sci. Technol. 5 (2008) 93–98.
[41] COMSOL, COMSOL Multiphysics Reference Manual Version 5.5, 2019.
[42] M.Th. van Genuchten, A closed-form equation for predicting the hydraulic conductivity of unsaturated soils, Soil Sci. Soc. Am. J. 44 (5) (1980) 892–898, https://doi.org/10.2136/sssaj1980.03615995004400050002x.
[43] M. Khamehchiyan, A. Hossein Charkhabi, M. Tajik, Effects of crude oil contamination on geotechnical properties of clayey and sandy soils, Eng. Geol. 89 (3–4) (2007) 220–229, https://doi.org/10.1016/j.enggeo.2006.10.009.
[44] U.S. Environmental Protection Agency, Quality Criteria for Water 1986, Report 440/5-86-001, 1986.
[45] MENV, Critères de qualité de l'eau de surface au Québec, Direction du suivi de l'état de l'environnement. Ministère de l'Environnement, Québec, QC, 2001.
[46] J. Bai, X. Ye, J. Jia, G. Zhang, Q. Zhao, B. Cui, X. Liu, Phosphorus sorption-desorption and effects of temperature, pH and salinity on phosphorus sorption in marsh soils from coastal wetlands with different flooding conditions, Chemosphere 188 (2017) 677–688, https://doi.org/10.1016/j.chemosphere.2017.08.117.
[47] R.H. Kadlec, S. Wallace, Treatment Wetlands, CRC Press, 2008, https://doi.org/10.1201/9781420012514.
[48] V. Cucarella, G. Renman, Phosphorus sorption capacity of filter materials used for on-site wastewater treatment determined in batch experiments—a comparative study, J. Environ. Qual. 38 (2) (2009) 381–392, https://doi.org/10.2134/jeq2008.0192.
[49] L. Johansson Westholm, Substrates for phosphorus removal—potential benefits for on-site wastewater treatment? Water Res. 40 (1) (2006) 23–36, https://doi.org/10.1016/j.watres.2005.11.006.
[50] R. Roseth, Shell sand: a new filter medium for constructed wetlands and wastewater treatment, J. Environ. Sci. Health A 35 (8) (2000) 1335–1355, https://doi.org/10.1080/10934520009377039.
[51] S.S. Dalahmeh, Y. Stenström, M. Jebrane, L.D. Hylander, G. Daniel, I. Heinmaa, Efficiency of iron- and calcium-impregnated biochar in adsorbing phosphate from wastewater in onsite wastewater treatment systems, Front. Environ. Sci. 8 (2020), https://doi.org/10.3389/fenvs.2020.538539.
[53] R. Samsó, J. García, P. Molle, N. Forquet, Modelling bioclogging in variably saturated porous media and the interactions between surface/subsurface flows: Application to Constructed Wetlands, J. Environ. Manag. 165 (2016) 271–279.
[54] Veillette, J. J., Paradis, S. J., & Buckle, J. (2005). *Bedrock and surficial geology of the general area around Rouyn-Noranda, Quebec and Ontario.*
[55] Geological Survey of Canada. (2014). *Surficial geology of Canada, Canadian Geoscience Map 195 (preliminary, Surficial Data Model v. 2.0 conversion of Map1880A), scale 1:5 000 000.*
[56] Geological Survey of Canada. (2019). Maps of surficial deposits. *1639A; 1640A; 1641A; 1642A; 1643A; 1644A; 1991A; 1992A; 1995A; 1996A; 2017A; 2018A; 2019A.*